J Mater Sci (2011) 46:1167–1175
DOI 10.1007/s10853-010-4888-3

Probing of wood–cement interactions during hydration of wood–cement composites by proton low-field NMR relaxometry

Y. A. M. Cheumani · M. Ndikontar · B. De Jéso · G. Sèbe

Received: 5 July 2010 / Accepted: 28 August 2010 / Published online: 14 September 2010

Abstract Proton NMR T_2 relaxometry has been applied to investigate phenomena involved in wood–cement composites during hydration. The transformation of capillary pore water into hydrates and gel pore water, as well as the microstructural changes occurring in the cement matrix, was continuously monitored during the first 28 days of hydration. Water in wood and its transfer into the matrix as cement hardens were also evidenced with the method. It has been found, for example, that some of the water in the mixture is retained in wood in the form of bound or free water, depending on the initial water content. By measuring the area under the different peaks, the consumption of water during hydration can be measured and the advancement of the hydration process can be evaluated via the hydration advancement coefficient α. The cement hardening within the composite has been also studied in the presence of calcium chloride, an accelerating agent. The acceleration was clearly evidenced at the early stage of the hydration process. The influence of extractives has been evaluated by comparing the hydration behaviour of composites prepared from *Eucalyptus saligna* (low extractives content) and *Afzelia bipendensis* (high extractives content), and a new compatibility index based on NMR relaxometry measurements has been proposed.

Y. A. M. Cheumani · B. De Jéso · G. Sèbe (✉)
Unité Sciences du Bois et des Biopolymères,
Université Bordeaux 1, Talence, France
e-mail: g.sebe@us2b.u-bordeaux1.fr

Y. A. M. Cheumani · M. Ndikontar
Laboratoire de Physico-Chimie du Bois,
Université de Yaoundé I, Yaoundé, Cameroun

Introduction

Wood–cement composites are a class of construction materials made by binding together wood particles or fibres with cement paste or mortar. These include composites prepared from non-wood agricultural fibres (e.g. sisal, bamboo, kenaf and flax) and other lignocellulosic wastes (e.g. bagasse, wheat straw, paper mill sludge, newspaper…) [1, 2]. These materials possess interesting properties such as thermal and acoustical insulation properties, fire resistance, fungi and termite resistance [3–5]. Numerous products are already on the market, but the industry is expected to grow further since the raw materials are available locally in many countries, and there is an increasing need for low-cost, durable and reduced environmental impact building materials [6, 7].

To improve further the performances of these materials, several scientific challenges have still to be addressed. One problem concerns the lack of compatibility between the cement and many wood species. The cement paste sets and hardens through a series of physico-chemical processes in contact of water [8–10]. These processes are sometimes inhibited when wood is added, depending on the species. This phenomenon is generally assigned to the diffusion of wood extractives or other substances resulting from the alkaline degradation of the lignocellulosic polymers (e.g. sugars, phenolic compounds, fatty acids…) [11–13]. Another problem is related to the hygroscopic character of wood. The absorption/desorption of water by wood components causes dimensional variations that limit the spectrum of application of this type of material [14–17]. The third problem concerns the weakening of wood fibres by alkaline attack and by fibre mineralization, which leads to the reduction of mechanical strength and toughness in the long term [18, 19].

A lot of efforts have been made in recent years to improve the material performances [20, 21], but the mechanisms involved during the cement hydration are still not totally understood, due to a lack of adequate methods of characterization. The classification of wood species according to their compatibility with cement is generally based on the measurement of the heat released during cement hydration [22–25]. This method gives only information on global cement hydration advancement, and the classification depends on the assessment scheme procedure applied (Inhibition index I, C_A factor…) [25, 26]. Mechanical testing can also help in estimating the level of compatibility between wood and cement, but it informs mostly on the global cohesion of the material [27, 28]. Other techniques have occasionally been used to characterize the wood/cement system: electrical conductivity measurements [29], X-ray diffraction [30], thermogravimetric analysis [30, 31], scanning electron microscopy [32, 33] and mercury intrusion porosimetry [34, 35], but all these techniques have also their own limitations (special sample preparation procedure, long implementation, only partial information…).

In this context, a new characterization method based on proton low-field NMR relaxometry has been developed. NMR relaxometry is a powerful non-destructive technique that can provide information about the evolution of the wood/cement system during hydration, through the analysis of water transformation and transfers within the composite. The technique can be also used to measure the interactions between the hardened material and the water found in its environment.

Proton NMR relaxometry or time-domain NMR has already been used by many authors to study the evolution of water in cementitious materials [36–42] or in wood [43–48]. Measurements of the signal amplitude and spin–lattice T_1 relaxation time, or spin–spin T_2 relaxation time, can be related to different material parameters such as moisture content and distribution [36–48], surface area [36, 47, 49] and pore-size distribution [50, 51]. In wood, the ^{1}H NMR signal from water can be separated on the basis of spin–spin T_2 relaxation times into cell-wall bound water (low T_2) and free water in the lumens (high T_2) [43–47]. The intensity of each signal is proportional to the number of protons at the corresponding T_2 relaxation time. In the cement, it is also possible to differentiate the water chemically bound into the hydrates structures from the free water filling the pores (gel pores and capillary pores, respectively) [36–42]. By using the fast exchange model, the relaxation times T_1 or T_2 of the water filling a pore can be also related to the pore dimensions [45, 50, 51].

In this article, we report a comprehensive method for the investigation of wood–cement systems during hydration, based on the measurement of the proton spin–spin T_2 relaxation time of water. The effectiveness of this approach to investigate the wood–cement compatibility and also the water transfers in the material during setting and hardening is clearly demonstrated.

Materials and methods

Raw materials

The cement used in this study was a commercial white Portland cement CEMI 52.5N (by European standard EN 197-1) supplied by Calcia cements. The low paramagnetic content of white cement makes it ideal for NMR experiments. Deionized water obtained from a Millipore® SWRE Mill-Q water purification system was used for all experiments. Two wood species were used: *Eucalyptus saligna* and *Afzelia bipendensis* (Doussie). Wood slices were cut into small chips and then ground in a Retsch SM 100 mill. The fraction of ground wood retained between 0.40- and 1.00-mm standard AFNOR sieves was used. Extracted wood was obtained *via* Soxhlet-extraction, first with toluene-ethanol (2:1 v/v) then with water. Each extraction lasted 8 h at the rate of six syphons an hour. After extraction, wood was air-dried and then oven-dried at 105 °C to constant weight. Dry wood samples were stored in a chamber conditioned at 25 °C and 75% relative humidity until use. Their equilibrium moisture content was then approximately 11–12%. In this study, each experiment was conducted in three replicates.

Low-field NMR relaxometry

Equipment

A Bruker Minispec NMS120 analyser operating at 20 MHz proton resonant frequency was used with a 10 VTS-GRA NMR probe. The typical dead time was set at 7 µs. This probe uses a 10-mm outer diameter NMR tube. The sensitive region in the RF coil is at 15–20 mm height. The maximum height of the sample in the tube was then adjusted to approximately 15 mm; the entire sample could thus be investigated. The temperature in the probe was maintained at 20 °C by a water circuit.

Sample preparation

Cement paste was prepared by thoroughly mixing 10 g of cement powder with water in a polyethylene bag for about 3 min. The amount of mixing water is given by a water-to-cement mass ratio (w/c). Part of the cement slurry obtained was poured into the NMR tube. The tube was conditioned in a water bath at 20 °C before and after the analysis.

To study wood–water interactions, wood powders were conditioned at 25 °C in a chamber containing a saturated aqueous NaCl salt solution (75% RH) or simply water (100% RH) to obtain wood samples with 12% or 28% of water, respectively (i.e. below the FSP). To obtain moisture contents above the FSP, water was directly mixed with wood, which was previously conditioned at 100% RH.

Wood–cement composites were prepared by first mixing wood sawdust with the dry cement. Water was then added and the system was homogenized manually. The wood-to-cement mass ratio (w_0/c) was fixed at 0.2 (on oven dry basis). A part of the composite obtained was directly poured into the NMR tube and conditioned at 20 °C. All the samples were capped to avoid any exchange with their environment.

Measurements

Spin–spin T_2 relaxation experiments were performed using the Carr–Purcell–Meiboom–Gill (CPMG) pulse sequence: $90^\circ_x - \left(\tau - 180^\circ_y - \tau\right)_n$ –RD with $n = 600$ and an echo time $2\tau = 200$ µs. This echo time is long enough to permit only the detection of liquid-phase protons in cement and wood. The solid-phase protons indeed relax at T_2 relaxation times (≈ 20 µs) too short to be detected in this case. A minimum of 256 scans were used with a recycle delay of 3 s. The T_2 distribution was obtained by resolving the magnetization signal decay using the CONTIN program by Provencher.

Calorimetry

Equipment

We used a 1-L Dewar flask, a Type J thermocouple and a Testo 177-T4 data collector. The collector was programmed to record temperature at 15-min intervals.

Sample preparation

The measurements were conducted on samples containing 100 g of cement, 20 g of wood and 50 g of water ($w_0/c = 0.2$ and $w/c = 0.5$). After mixing wood with the cement in a polyethylene bag, water was added and the system was homogenized manually. A thermocouple was introduced in the middle of sample and connected to the data collector. The sample bag was then placed in Dewar flask and the flask was sealed. The entire operations were rapidly executed, so as to get the first measurement as soon as possible. The ambient temperature was averagely 22 ± 2 °C.

Results and discussion

Hydration of the neat cement

The proton spin–spin T_2 relaxation measurements were performed using the Carr–Purcell–Meiboom–Gill (CPMG) spin echo sequence, which allows, when applied with an echo time sufficiently long, the observation of the mobile water in the material. The recorded magnetization signals were analysed with an inverse Laplace transformation performed numerically with the CONTIN program. Previous study showed that this program is more stable for the analysis of multi-exponentials decay signals containing up to five components [52, 53].

Before analysing the wood–cement system, preliminary experiments were conducted with the neat cement matrix. The cement paste P1 was prepared with a water-to-cement weight ratio (w/c) of 0.5, and the evolution of the spin–spin T_2 relaxation time of the system was recorded during hydration (Fig. 1). White cement was used to limit the impact of the paramagnetic oxides found in the commercial ordinary Portland cements (e.g. ferric oxides, responsible for the grey colour). These oxides can accelerate the spin–spin relaxation, leading to very short relaxation times difficult to analyse. At the beginning of the hydration process (0.5 h after mixing), only one intense signal is observed at about 15–43 ms and is assigned to the water in the larger pores of the cement, i.e. the capillary pores [36, 41]. As the hydration proceeds, this peak is shifted towards lower relaxation times (its intensity decreases also), and a new peak assigned to the water in the gel pores (smallest pores of the cement) emerges at about 0.1–0.8 ms. Since the peak position depends on the water molecules mobility, a high mobility causes low spin–spin interaction and high T_2 values. It has been shown, using the fast exchange model, that the T_2 of the water filling a pore can be related to the pore dimensions according to the following expression (Eq. 1) [50, 51]:

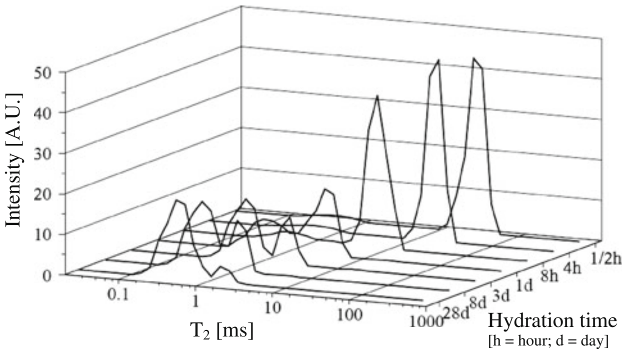

Fig. 1 Distribution and evolution of the spin–spin T_2 relaxation times during hydration of the neat cement paste P1 (w/c = 0.5). *A.U.* arbitrary units

$$\frac{1}{T_{1,2\text{mes}}} = \frac{S}{V}\frac{\lambda}{T_{1,2\text{suf}}} \quad (1)$$

where $T_{1,2\text{mes}}$ is the $T_{1,2}$ measured; $T_{1,2\text{surf}}$ is the $T_{1,2}$ at the pore surface; λ is the thickness of the protons surface layer; S is the pore surface and V is the pore volume.

Therefore, when the pore size decreases, T_2 decreases. The decrease in the size of capillary pores is very fast between 2 and 8 h, as illustrated by the fast downshift of the $T_{2\text{cap}}$ signal during this period (Fig. 2). This decrease coincides with the high increase in temperature inside the cement, which is maximal after 8 h (Fig. 2). During this process, capillary pores are progressively filled by the hydration products (i.e. calcium silicate hydrates, portlandite and ettringite), leading to a progressive decrease in the pore sizes. This so-called 'acceleration period' (setting period) is in fact a period where bridges are built between cement grains, leading to a reduction of water mobility *via* the compartmentalization of the capillary spaces. Between 8 and 24 h, the size of capillary pores continues to decrease, but much more slowly. After 24 h, the modification of the pores size is only marginal, the T_2 of capillary pores stabilizing at a constant value of about 0.8–2.4 ms. The peak of gel water on the other hand (~0.1–0.8 ms) is not significantly displaced during the whole hydration process (but its intensity increases with time). The peak amplitude being proportional to the water population at the T_2 considered, the peak area gives an estimation of the water content in the capillary pores (W_{cap}) and gel pores (W_{gel}) at each stage of the hydration process (Fig. 3). By summing the areas under the different peaks, the total water content (W_{tot}) can be also calculated (Fig. 3). The kinetics of the hydrates formation can then be estimated from the consumption of the W_{tot} water during hardening. In Fig. 3, nothing happens during the first 2 h after mixing, i.e. during the so-called 'dormant period' characterized by a near or total absence of chemical processes [54, 55]. After 2 h, the capillary water content (W_{cap}) starts to decrease as the water content in the gel pores (W_{gel}) concomitantly increases. Accordingly, part of the capillary water is progressively converted into gel water, but also into hydration products since the total water content decreases with time (W_{tot} in Fig. 3). The hydration advancement $\alpha(t)$, defined as the fraction of cement that is fully hydrated, can be deduced from the evolution of W_{tot} using Eq. 2 [40]:

$$\alpha(t) = \frac{(w/c)}{(w/c)_0}(100 - W_{\text{tot}}(t)) \quad (2)$$

where (w/c) is the water-to-cement weight ratio, $(w/c)_0$ the amount of water chemically bonded per gram of cement at full hydration and $W_{\text{tot}}(t)$ the total water content at the hydration time t. In the literature, the $(w/c)_0$ value is estimated at 0.23 [56, 57]. The evolution of α during the hydration of the cement paste P1 is reported in Fig. 3. Hence, approximately 70% of the cement is hydrated in P1 after 28 days. We should mention that full cement hydration (i.e. $\alpha = 100\%$) can take years.

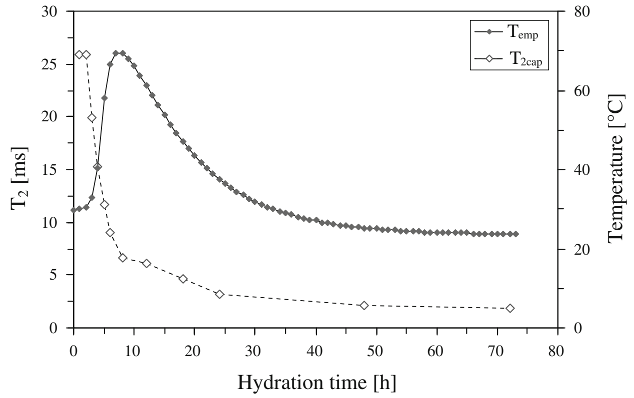

Fig. 2 Evolution of the capillary water T_2 ($T_{2\text{cap}}$) during the first 3 days of hydration for the paste P1 (w/c = 0.5; left y-axis). The evolution of cement temperature (T_{emp}) is also reported (right y-axis)

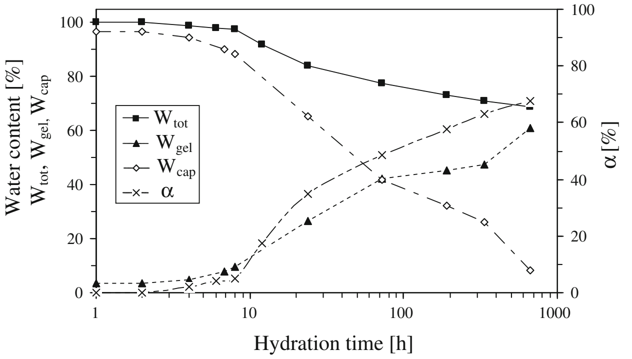

Fig. 3 Evolution of the different water contents measured by relaxometry, during the first 28 days of hydration for the paste P1 (w/c = 0.5). W_{cap}: capillary water; W_{gel}: water in the gel pores; W_{tot}: total water content; α: hydration advancement

Distribution of water in wood

In preliminary experiments, *E. saligna* was chosen as the wood species to study the wood–cement system by ^{1}H NMR relaxometry. Wood particles (0.4–1 mm) were first analysed without the cement: wood was conditioned in varied humid environments and the spin–spin T_2 relaxation times of the samples were recorded. Results obtained with extracted *E. saligna* are shown in Fig. 4 (similar spectra were obtained with unextracted samples).

In wood, the water NMR signal can be separated into bound water ($T_2 \sim 1$ ms; water adsorbed in the cell-wall by hydrogen bonding) and free water ($T_2 \sim 10$–100 ms; water in the cell-wall lumen) [43–47]. The intensity of each

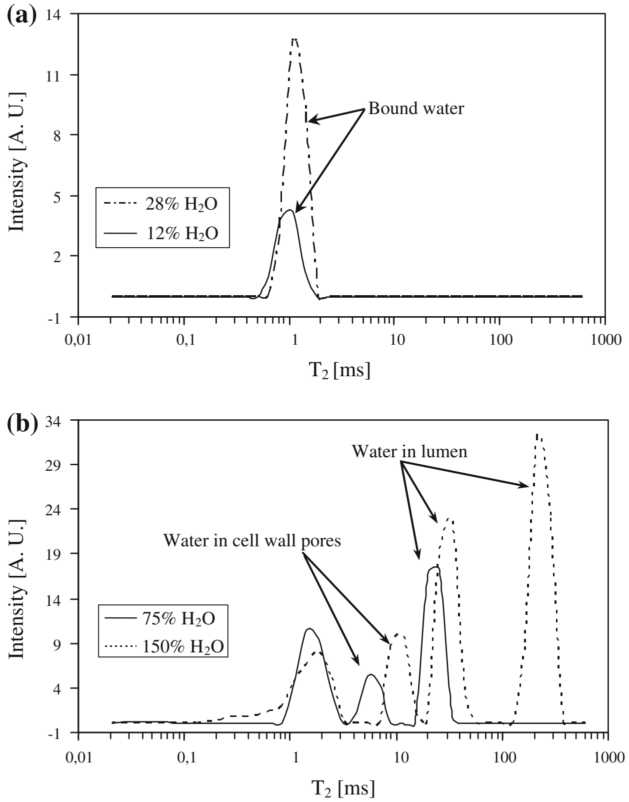

Fig. 4 T_2 distribution of water in extracted *Eucaltyptus saligna* wood samples of different water contents (w/w %): **a** Below FSP; **b** above FSP

signal is proportional to the number of protons at the corresponding T_2 relaxation time. Below the fibre saturation point (FSP), only the T_2 component corresponding to bound water is observed, at about 0.8–1.4 ms (Fig. 4a). Above the FSP, three or four T_2 components are observed, depending on the moisture content (Fig. 4b). The first component ($T_2 \sim$ 0.8–2.4 ms) corresponds to bound water and the others to free water. According to the fast exchange model, there is a correlation between the T_2 of water and the pores size in wood [45]. Therefore, we can deduce from Fig. 4b that *E. saligna* contains three types of pores, the larger pores being filled only when the water content in wood is sufficiently high (i.e. 150% in Fig. 4b). The T_2 at 4.1–6.9 ms has been assigned to the small pores found in the cell-wall [58, 59], the T_2 at 19.9–43.7 ms to the wood cell lumens (i.e. fibres, parenchyma or rays) and at 164–279 ms to the wood vessels.

Hydration of the wood–cement composites

Analysis of composite C1 ($w/c = 0.5$; $w_0/c = 0.2$)

The first wood–cement composite studied (composite C1) was prepared with extracted *E. saligna* sawdust, using a water-to-cement weight ratio (*w/c*) of 0.5 and a wood-to-cement weight ratio (*w*$_0$*/c*) of 0.2.

Figure 5 shows the evolution of the different T_2 during hydration of the composite C1. After 0.5 h, two peaks assigned to bound water in wood ($T_2 \sim$ 0.8–4.1 ms; large signal) and capillary water in cement ($T_2 \sim$ 4.1–25.9 ms) are observed. As in neat cement, the temperature of the system increases rapidly as the T_2 of capillary water shifts towards lower relaxation times, the capillary pores being progressively filled by the hydration products. Concomitantly, the T_2 corresponding to the water in the gel pores emerges and starts to be clearly visible after 8 h ($T_2 \sim$ 0.1–0.8 ms; its intensity increases with time). After 4 h, the capillary water signal shifted below 10 ms and the free water present in the wood lumens can now be observed, at about 11.7–25.9 ms. The intensity of this peak starts to decrease after 8 h, indicating that this water is progressively transferred into the cement matrix during hydration. After 3 days, the wood lumens are quasi-empty and we only observe a small signal corresponding to the free water of the cell-wall pores at about 5.3 ms. After 28 days, the spectrum is similar to what was observed with neat cement (Fig. 1) except that the peak intensity at 1.1–2.4 ms is more important, due to the contribution of the bound water in wood expected in the same area (the peaks of capillary water in cement and bound water in wood overlap).

The evolution of W_{tot}, W_{gel} and W_{cap} during the hydration of C1 is given in Fig. 6. After 28 days, W_{cap} is higher in C1 than in P1 (7% in P1 and 29% in C1), but the total water content is similar in both materials (~70% of the water introduced initially). The water content in the capillary pores of the cement in C1 is probably overestimated since the bound water in wood contributes to this signal (the peaks overlap). W_{gel} on the other hand is lower in the composite (63% in P1 and 43% in C1), probably because

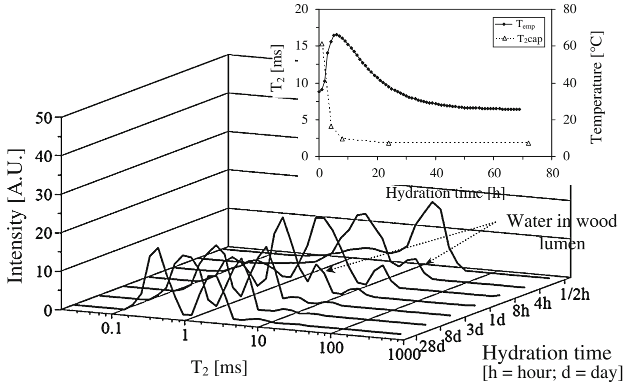

Fig. 5 Distribution and evolution of the different T_2 during hydration of the composite C1 (w/c = 0.5 and w_0/c = 0.2). The inset gives the evolution of the capillary water T_2 (T_{2cap}) and cement temperature (T_{emp}) during the first 3 days of hydration

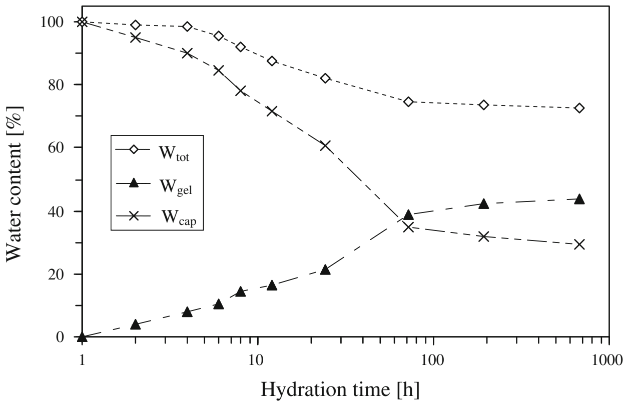

Fig. 6 Evolution of the different water contents measured by relaxometry, during the first 28 days of hydration for the composite C1 ($w/c = 0.5$ and $w_0/c = 0.2$). W_{cap}: capillary water; W_{gel}: water in the gel pores; W_{tot}: total water content

wood retains water and modifies the microstructure of hydrates.

Impact of initial water content

The evolution of the wood–cement system during hydration was studied as a function of *w/c* (initial mixing water content), the wood-to-cement weight ratio w_0/c being maintained at 0.2. The evolution of T_2 relaxation time of the capillary water in the composites prepared with different initial water content is presented in Fig. 7 (*w/c* = *0.3, 0*.5 and *0.8* in composites C2, C1 and C3, respectively). The evolution of α is also reported.

Compared with C1, the T_2 of capillary water at the beginning of the hydration process is higher in C3 and lower in C2 (Fig. 7a). Indeed, as *w/c* decreases, the spaces between cement grains also decreases, which restricts the mobility of water (T_2 is smaller). In all the composites, T_2 shifts towards lower values as the cement hardens, and stabilizes at about 1–3 ms (after 8 h in the case of C1 and C2, after 72 h in the case of C3). After 28 days of hydration, α is about two times lower in C2 than in C1 or in C3, indicating that the initial water content has a strong impact on the hydration rate. When the initial water content is too low, the hydration is slow and stops prematurely (α ~ 30% after 28 days in the case of C2). The wood pores in such composites remain empty after 28 days since only bound water is detected (Fig. 8a). Conversely, when the initial water content is high, free water is observed in the wood lumens and cell-wall pores inside the composite (Fig. 8b).

Impact of $CaCl_2$ as accelerating agent

Wood–cement composites were prepared in the same conditions than with C1, but in the presence of calcium chloride, an accelerating agent commonly added in the formulations to reduce the setting time and improve the mechanical performance [20, 60]. Figure 9 shows the evolution of α during hydration of the composite C4 prepared with a water-to-cement weight ratio (*w/c*) of 0.5, a wood-to-cement weight ratio (w_0/c) of 0.2 and a $CaCl_2$-to-cement weight ratio ($CaCl_2/c$) of 0.04. The relaxometry results show clearly that $CaCl_2$ accelerates the hydration process as soon as water is added in the system since the 'dormant period' (α = 0 during the first 4 h with C1) is no longer observed with C4. We also observed an acceleration of the water transfer from the wood particles to the cement matrix during hydration, the intensity of the peak associated to the free water in wood decreasing faster in the presence of $CaCl_2$ (results not shown). The gel water content was also slightly lower in C4 than in C1 after 28 days, maybe because of some microstructural changes induced by the presence of $CaCl_2$.

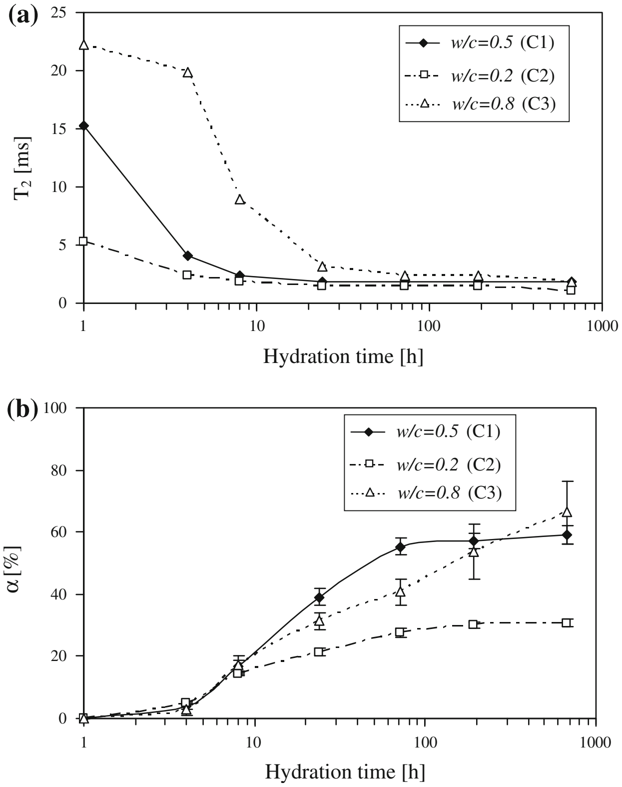

Fig. 7 Evolution during hydration of **a** T_2 relaxation time of capillary water and **b** hydration advancement coefficient α, for the composites prepared with different initial water contents (*w/c* = 0.3, 0.5 or 0.8)

Impact of extractives

It has been shown that the extractives compounds (such as sugars or tannins) present in wood can inhibit the hydration process. They migrate in alkaline cement medium and block hydrates nucleation and growth by adsorption on the

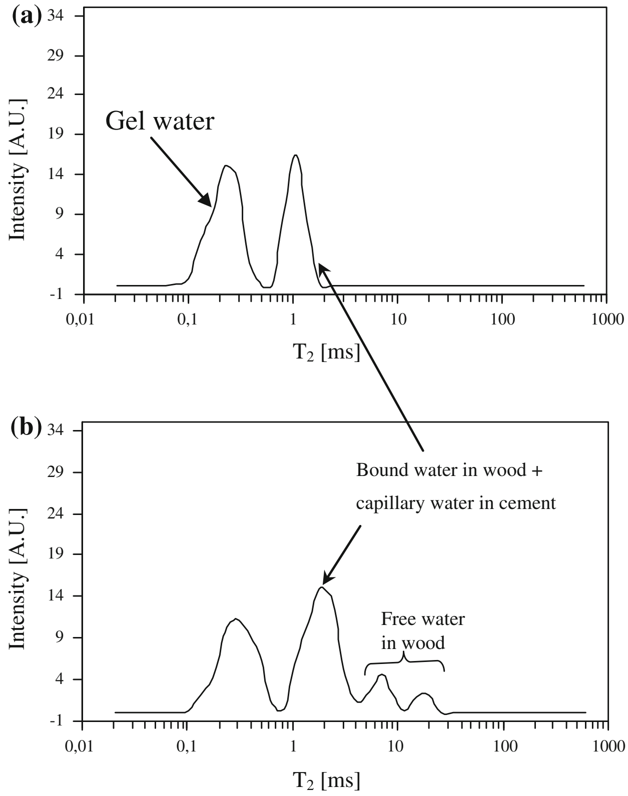

Fig. 8 T_2 distribution of water in **a** composite C2 (w/c = 0.3 and w_0/c = 0.2) and **b** composite C3 (w/c = 0.8 and w_0/c = 0.2), after 28 days of hydration

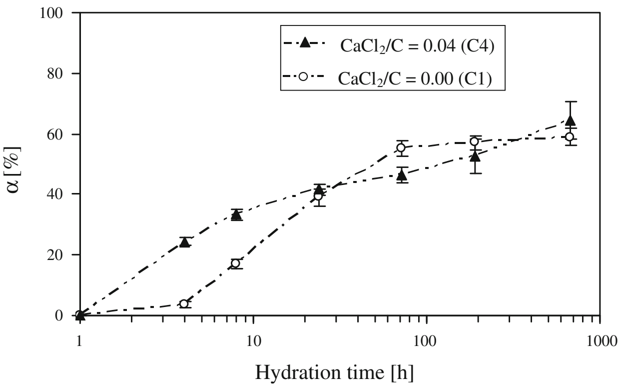

Fig. 9 Influence of $CaCl_2$ on the hydration of wood–cement composites (w/c = 0.5 and w_0/c = 0.2) (α = hydration advancement coefficient determined by NMR)

surface of the cement grains or by complexation of the ionic metallic species found in the cement. The removal of extractives could solve this problem but the operation is expensive, so unextracted wood is generally preferred. Some species being more compatible than others, depending on the extractives nature and content, it is necessary to classify wood according to their compatibility with cement. This classification is generally based on the measurement of the heat released during cement hydration [23–26], but the ^{1}H NMR relaxometry could serve as an alternative method. Therefore, the compatibilities of *E. saligna* and *A. bipendensis* with cement were compared by NMR relaxometry. These two Cameroonian wood species having very different extractives content, different behaviour should be observed. After extraction with toluene/ethanol (2/1 v/v) and then with water, the extractives content was found to be 2.8% for *E. saligna* and 20.5% for *A. bipendensis*. Figure 10 shows the evolution of α during the first 3 days of hydration for the composites prepared form *E. saligna* (C5) and *A. bipendensis* (C6), with a water-to-cement weight ratio (w/c) of 0.5 and a wood-to-cement weight ratio (w_0/c) of 0.2. The evolution of the cement temperature (T_{emp}) is also reported (right y-axis).

As expected, the extractives of *E. saligna* have no notable impact on the evolution of α during hydration, at least during the first 3 days of hydration (comparison with α in Fig. 3). With *A. bipendensis* on the other hand, the high extractives content led to total inhibition of the cement hydration (α ~ 0 after 3 days). The relaxometry results are in good agreement with the temperature profiles measured by calorimetry since no exothermic peak was measured in the case of C6, confirming the absence of hydration reactions in that composite (Fig. 10, right axis).

The relaxometry method can therefore be used to classify wood species according to their compatibility with the cement. Based on the hypothesis that, for wood–cement samples prepared in the same conditions, the most compatible wood species is the one that leads to the highest hydration advancement at a given hydration time t, a new compatibility index I_{NMR} is proposed (Eq. 3):

$$I_{\mathrm{NMR}}(\%) = \frac{\alpha_{\mathrm{composite}}(t)}{\alpha_{\mathrm{cement\ paste}}(t)} \times 100 \qquad (3)$$

The I_{NMR} after one day of hydration is for example 93% and 0% for *E. saligna* and *A. bipendensis*, respectively.

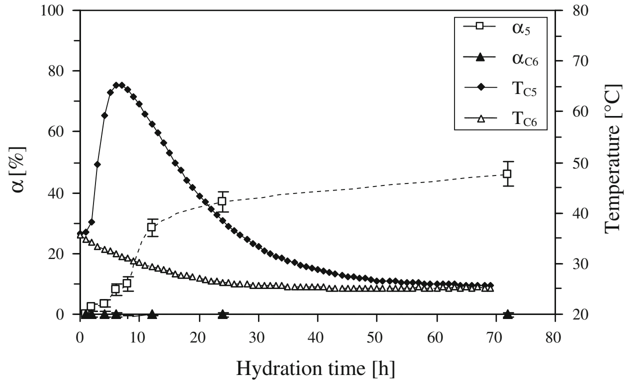

Fig. 10 Evolution of the hydration advancement coefficient α and temperature T for the composites prepared form *Eucalyptus saligna* (C5) and *Afzelia bipendensis* (C6), with w/c = 0.5 and w_0/c = 0.2 (unextracted sawdust)

Conclusion

Proton NMR relaxometry has been used to investigate phenomena involved in wood–cement composites during setting and hardening. The spectra of neat cement paste show the presence of two T_2 components corresponding to two different water populations within the material: gel and capillary water. The evolution of relaxation time T_2 and the intensity of each type of water give information about the water consumption and microstructural changes during hydration. Four types of water have been identified in wood depending on its moisture content: bound water, free water present in the cell-wall pores, the lumen and the vessels. In wood–cement composites, it was observed that, in addition to phenomena associated to cement hydration, there is migration of water, especially free water, from wood to the cement matrix. At the end of the process, some of the water is retained in wood, in the form of bound or free water, depending on the initial water content. By measuring the area under the different peaks, it was possible to calculate the hydration advancement coefficient α at each stage of the process, which can be used to assess the compatibility of the wood species with cement. The difference in the behaviour of cement in the presence of *E. saligna* (compatible wood) and *A. bipendensis* (incompatible wood) has been clearly observed, and a new compatibility index based on NMR relaxometry measurements has been proposed. The technique proved also to be effective at evaluating the impact of admixture (such as accelerating agents) or extractives on the hydration process. In conclusion, the NMR relaxometry technique is a powerful tool to monitor the hardening process during the elaboration of wood–cement composites or the optimization of the systems.

Acknowledgements This study is part of Arnaud Cheumani's Ph.D. thesis. We wish to thank the AUF 'Agence Universitaire de la Francophonie', and US2B-University Bordeaux 1 for their financial support. We are grateful to Calcia cements for gracefully providing Portland cement samples.

References

1. Moslemi AA (1997) Inorganic-bonded wood and fiber composite materials. Forest Prod Soc, Madison
2. Sobral HS (1990) Proceedings of the second international Rilem symposium, held in Salvador, Bahia, Brazil, September 17–21, 1990. Chapman & Hall, London
3. Durisol-Material properties. http://www.durisolbuild.com/webdocs/durisol%20material%20properties.pdf. Accessed 3 April 2010
4. Avis technique 16/05-487 Agreslith-C/Société Agresta. http://tbd-atec.cstb.fr/fichiers/pdf/GS16-Q/AQ05487.pdf. Accessed 3 April 2010
5. Avis technique 2/09-1337 Duripanel/Eternit. http://tbd-atec.cstb.fr/fichiers/pdf/GS02-C/AC091337.pdf. Accessed 3 April 2010
6. Moslemi AA (1999) Adv Perform Mater 6:161
7. Ramirez-Coretii A, Eckelman CA, Wolfe RW (1998) Forest Prod J 48:62
8. Taylor HFW (1997) Cement chemistry, 2nd edn. Thomas Telford, London
9. Older I (1998) Lea's chemistry of cement and concrete, 4th edn. Elsevier
10. Moir G (2003) In: Newman J (ed) Cement in advanced concrete technology constituents materials. Elsevier
11. Sandermann W, Preusser HJ, Schwiens W (1960) Holzforchung 14:70
12. Miller DP, Moslemi AA (1991) Wood Fiber Sci 23:472
13. Semple KE, Cinningham RB, Evans PD (2004) Wood Fiber Sci 36:250
14. Mougel E, Beraldo AL, Zoulalian A (1995) Holzforschung 49:471
15. Fan MZ, Bonfield PW, Dinwoodie JM, Breese MC (1999) Cement Concrete Res 29:923
16. Ledhem A, Dheilly RM, Benmalek ML, Queneudec M (2000) Can J Civil Eng 27:101
17. Rudkiewicz F (2001) Procédé de traitement d'un granulat de bois ou autre matériau organique fibreux entrant dans la fabrication d'un composite à base de ciment. Patent WO/2001/0607759
18. Tolêdo Filho RD, Scrivener K, England GL, Ghavami K (2000) Cem Concr Compos 22:127
19. Mohr BJ, Biernacki JJ, Kurtis KE (2006) Cem Concr Res 36:240
20. Jorge FCP C, Ferreira JMF (2004) Holz und Roh-Werkstoff 62:370
21. Frybort S, Mauritz R, Teischinger A, Müller U (2008) BioResources 3(2):602
22. Sandermann W, Kohler R (1964) Holzforschung 18:53
23. Hachmi M, Moslemi AA, Campbell AG (1990) Wood Sci Technol 24:345
24. Sauvat N, Sell R, Mougel E, Zoulalian A (1999) Holzforschung 53:104
25. Karade SR, Irle M, Maher K (2003) Holzforschung 57:672
26. Olorunnisola AO (2007) Cem Concr Compos 30:37
27. Lee AWC, Hong Z (1986) For Prod J 36:87
28. Blankenhorn PR, Labosky P Jr, DiCola M, Stover LR (1994) For Prod J 44:59
29. Govin A, Peschard A, Fredom E, Guyonnet R (2005) Holzforchung 59:330
30. Vaickelionis G, Vaickelioniene R (2006) Ceramics-Silikáty 50:115
31. Govin A, Peschard A, Guyonnet R (2006) Cem Concr Compos 28:12
32. Fujii T, Miyatake A (2003) Bull Forestry Forest Prod Res Inst 2:93
33. Wei YM, Fujii T, Hiramatsu Y, Miyatake A, Yoshinaga S, Fujii T, Tomita B (2004) J Wood Sci 50:327
34. Bouguerra A, Ledhem A, de Barquin F, Dheilly RM, Queneudec M (1998) Cem Concr Res 28:1179
35. Rodrigues CDS, Ghavami K, Stroeven P (2006) J Mater Sci 41:6925. doi:10.1007/s10853-006-0217-2
36. Halperin WP, Jehng JY, Song YQ (1994) Magn Reson Imaging 12:169
37. Bohris AJ, Goerke U, McDonald PJ, Mulheron M, Newling B, Le Page B (1998) Magn Reson Imaging 16:455
38. Holly R, Reardon EJ, Hansson CM, Peemoeller H (2007) J Am Ceram Soc 90:570
39. Faure PF, Rodts S (2008) Magn Reson Imaging 26:1183
40. Nestlé N (2004) Cem Concr Res 34:447
41. Gorce J-P, Milestone NB (2007) Cem Concr Res 37:310
42. Friedemann K, Schönfelder W, Stallmach F, Kärger J (2008) Mater Struct 41:1647

43. Menon RS, MacKay AL, Hailey JRT, Bloom M, Burgess AE, Swanson JS (1987) J Appl Polym Sci 33:1141
44. Araujo CD, MacKay AL, Hailey JRT, Whittall KP, Le H (1992) Wood Sci Technol 26:101
45. Xu Y, Araujo CD, MacKay AL, Whittall KP (1996) J Magn Reson B 110:55664
46. Hartley ID, Avramidis S, MacKay AL (1996) Wood Sci Technol 30:141
47. Haranczyk H, Weglarz WP, Sojka Z (1999) Holzforschung 53:299
48. Labbé N, De Jeso B, Lartigue JC, Daudé G, Pétraud M (2002) Holzforschung 56:25
49. Thomas JJ, Jennings HM, Allen AJ (1999) Concr Sci Eng 1:45
50. Bhattacharja S, Moukwa M, D'orazio F, Jehng J-Y, Halperin WP (1993) Adv Cement Based Mater 1:67
51. Philippot S, Korb JP, Petit D, Zanni H (1998) Magn Reson Imaging 16:515
52. Borgia GC, Bortolotti V, Brown RJS, Castaldi P, Fantazzini P, Soverini U (1994) Magn Reson Imaging 12:209
53. Labbé N (2002) Mise au point d'une méthode de dosage de l'eau dans le bois et caractérisation des composés organiques du pin maritime par résonance magnétique nucléaire domaine temps. Thèse de Doctorat, Université Bordeaux 1
54. Jolicoeur C, Simard M (1998) Cem Concr Res 20:87
55. Xu Q, Stark J (2005) Adv Cem Res 17:1
56. Neville AM (1981) Properties of concrete, 3rd edn. ELBS/Longman, London
57. Aligizaki KK (2006) Pore structure of cement-based materials: testing interpretation and requirements. Taylor & Francis, London
58. Topgaard D, Söderman O (2002) Cellulose 9:139
59. Persson PV, Hafrén J, Fogden A, Daniel G, Iversen T (2005) Biomacromolecules 5(3):1097
60. Ma LF, Yamauchi H, Pulido OR, Tamura Y, Sasaki H, Kawai S (2002) In: Evans PD (ed) Wood-cement composites in the Asia-Pacific region, Proceedings of a workshop held in Canberra, Australia, ACIAR Proceedings No. 107, pp 13–23